

# Low Temperature Power Cycle Using Amine – CO<sub>2</sub> Fluid

Takashi OGAWA<sup>1\*</sup>, Takashi MAWATARI<sup>1</sup>, Akira ITOH<sup>1</sup> and Yasushi YAMAMOTO<sup>1</sup>

<sup>1</sup>Energy Systems Research and Development Center, Toshiba Energy Systems & Solutions Corporation, 8 Shinsugita-cho, Isogo-ku, Yokohama, Kanagawa 235-8523, Japan

**Abstract** Low temperature heat below 473K is produced massively. Kalina cycle using NH<sub>3</sub> and Organic Rankine cycle using HFC-245fa can generate electricity from the low temperature heat. However, the former is toxic and corrosive and the latter has a high GWP value, which is required to reduce by the Kigali amendment to the Montreal Protocol and the Regulation (EU) No 517/2014. The thermodynamic simulation shows the maximum power of the low temperature cycle using 30 mass% MDEA-H<sub>2</sub>O solution (CO<sub>2</sub>/MDEA mole ratio: 0.15) is equal to that of the Organic Rankine cycle using HFC245fa. The experimental results suggest the low temperature cycle using the MDEA-based solution containing carbon dioxide is available as a low temperature cycle.

## 1 Introduction

Low temperature heat below 473K is produced massively (Shindo *et al.*, 2008). Kalina and Organic Rankine cycles can generate electricity from the low temperature heat. Ammonia used in Kalina cycle is toxic and corrosive. HFC-245fa (CHF<sub>2</sub>CH<sub>2</sub>CF<sub>3</sub>) used in Organic Rankine cycle has a global warming potential (GWP) value relative to carbon dioxide (CO<sub>2</sub>) of 858 (Myhre *et al.*, 2013). Therefore, the Kigali amendment to the Montreal Protocol and the Regulation (EU) No. 517/2014 require the reduction of such as HFC-245fa.

In carbon dioxide capturing systems, amine solutions absorb CO<sub>2</sub> at 313 K and the CO<sub>2</sub> partial pressure (P<sub>CO<sub>2</sub></sub>) of 0.01 to 10 kPa and desorb CO<sub>2</sub> at 393 K and P<sub>CO<sub>2</sub></sub> of 100 to 200 kPa (Ogawa *et al.*, 2008).

As a process that utilizes less toxic and low GWP working fluid, the present authors have proposed to amine-CO<sub>2</sub> absorption/desorption system for power generation.

## 2 Low Temperature Cycle Using Amine-CO<sub>2</sub> Fluid

### 2.1 Model

Figure 1 shows a low temperature cycle using amine-CO<sub>2</sub> fluid. An amine-CO<sub>2</sub>-H<sub>2</sub>O solution (S8) is pressurized in a pump (P1) and heated in a recuperator (Hx3) and a heater (Hx1). A H<sub>2</sub>O-CO<sub>2</sub> gas mixture (S11) desorbed from the heated amine-CO<sub>2</sub>-H<sub>2</sub>O solution (S12) and a residue (S13) are separated by a gas-liquid separator (Sep1). The H<sub>2</sub>O-CO<sub>2</sub> gas mixture (S11) drives turbine (EX1) and expands adiabatically. The residue (S13) heats a pressurized amine-CO<sub>2</sub>-H<sub>2</sub>O solution (S3).

The expanded H<sub>2</sub>O-CO<sub>2</sub> gas mixture (S5) and the residue (S14) cooled in the recuperator (Hx3) are mixed in a mixer (M1) and cooled to 313 K in a cooler (Hx2).

It is assumed that the values of the polytropic efficiency of P1, the isentropic efficiency of EX1, the pressure losses of Hx1, Hx2, Hx3, and Sep1 are 75%, 85%, 0kPa, respectively. The pinch temperatures of Hx1, Hx2, and Hx3 are assumed to be 4 K, 5 K, and 5 K, respectively. The vapor phase fraction at the EX1 outlet is more than 0.88 (Nishikawa, 1965). The pressure at the pump inlet is the minimum value when the vapor phase fraction is zero. The process simulator VMGSim<sup>TM</sup> v9.0 (Thermodynamic model: Amines) of the Virtual Materials Group Inc. simulated the model.

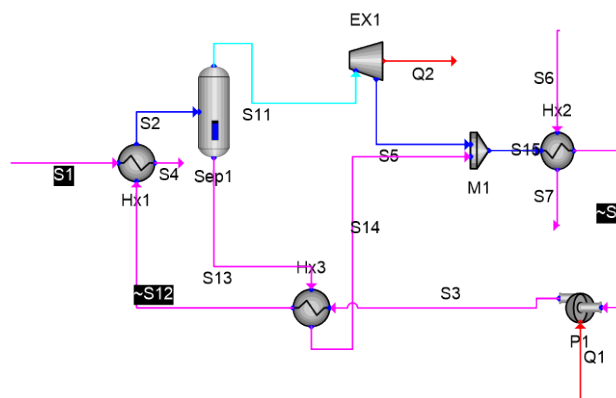


Figure 1. Low temperature cycle using amine-CO<sub>2</sub> fluid

### 2.2 Experimental

#### 2.2.1 Experimental equipment

\* Corresponding author: [taka.ogawa@toshiba.co.jp](mailto:taka.ogawa@toshiba.co.jp)

Figure 2 shows a schematic of the experimental equipment which verifies the low temperature cycle using amine-CO<sub>2</sub> fluid. The experimental equipment consists of a CO<sub>2</sub> absorber, a pump, a recuperator, a gas generator, a gas cooler, a separator, and so on. A CO<sub>2</sub> rich amine solution is pressurized in the pump (P) and heated in the recuperator and the gas generator. A gas mixture of CO<sub>2</sub> and H<sub>2</sub>O is generated in the gas generator. The gas mixture of CO<sub>2</sub> and H<sub>2</sub>O cooled in the gas cooler is separated into H<sub>2</sub>O liquid and CO<sub>2</sub> gas in the separator. A CO<sub>2</sub> lean amine solution discharged from the gas generator heats the CO<sub>2</sub> rich amine solution in the recuperator. The CO<sub>2</sub> gas is absorbed by the CO<sub>2</sub> lean amine solution in the CO<sub>2</sub> absorber.

The CO<sub>2</sub> absorber has the random packed bed whose diameter and height are 53.6 mm and 250 mm, respectively. The random packing is To-toku Engineering Corporation's Heli Pack No.2 whose porosity, specific surface area, and material are 92.6%, 3160m<sup>2</sup>/m<sup>3</sup>, and SUS316, respectively.

The amount of amine solution is 4 L (dm<sup>3</sup>). After vacuum evacuation using a stream ejector, the specified amount of CO<sub>2</sub> was injected using the small cylinder which contains CO<sub>2</sub> of 40 L at the normal temperature and pressure.

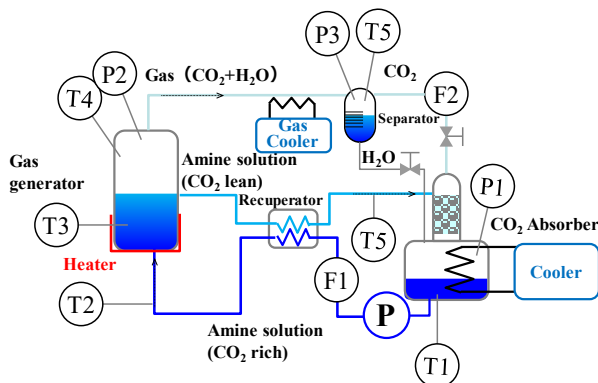


**Figure 2.** A schematic of the experimental equipment for the low temperature cycle using amine-CO<sub>2</sub> fluid  
F: Flow Rate, P: Pressure, T: Temperature

### 2.2.2 Estimation of work and efficiency

The work of the experimental equipment ( $W$  (W)) is calculated adiabatically using VMGSim's Expander unit, which utilizes the temperature of the gas mixture of CO<sub>2</sub> and H<sub>2</sub>O (T4), the pressure of the gas generator (P2), the steam flow rate using the separator, the CO<sub>2</sub> flow rate (F2), the pressure of the CO<sub>2</sub> absorber (P1), and the adiabatic efficiency of 100%. The steam flow rate was measured using a change of the water level in the separator. The pressure drop in the random paced bed was estimated below 7 Pa using the Ergun equation (Ergun, 1952; Akgiary and Saatci, 2001). This is much less than the pressure of the CO<sub>2</sub> absorber of about 10 kPa.

The heat input of the experimental equipment ( $Q$ ) is calculated as follows:

$$Q = Q_H - Q_R \quad (1)$$

where  $Q_H$  is the input power of the heater (W) and  $Q_R$  is the heat loss from the experimental equipment(W).  $Q_R$  is evaluated using the heat balance of H<sub>2</sub>O circulation as follows:

$$Q_R = 1.45 T - 45.0 \quad (2)$$

where  $T$  is the temperature of the liquid phase in the gas generator (T3 (°C)). The efficiency ( $\eta$ ) of the experimental equipment was calculated as follows:

$$\eta = W/Q \quad (3)$$

## 3 Results and Discussion

### 3.1 Model predictions

The high temperature heat source is hot water whose temperature and flow are 368K and 75,000kg/h, respectively. At the same time Rankine and Organic Rankine (HFC245fa) cycles are evaluated for comparison.

Figure 3 shows the power as functions of expansion ratio and fluid flow at MDEA concentration of 30 mass percent and CO<sub>2</sub>/MDEA mole ratio of 0.15. The maximum power increases and its point moves to the lower expansion ratio with the fluid flow from 5,000 to 5,500 kg/h. Thereafter, the maximum power decreases and its point moves to the higher expansion ratio with the fluid flow.

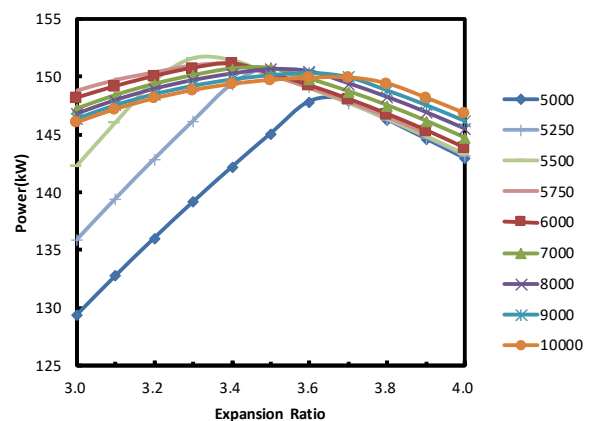


**Figure 3.** Power as functions of expansion ratio and fluid flow at 30 mass% MDEA and CO<sub>2</sub>/MDEA mole ratio of 0.15

Table 1 shows the maximum power dependency on the fluid, fluid flow, and expansion ratio.

The values of maximum power of 30 mass% methyl di-ethanolamine (MDEA)-H<sub>2</sub>O solutions show the highest one of 151 kW at the CO<sub>2</sub>/MDEA mole ratio of 0.15. The values of maximum power of ethanolamine (MEA)-H<sub>2</sub>O solutions are less than those of MDEA-H<sub>2</sub>O solutions.

The value of maximum power of 30 mass% MDEA-H<sub>2</sub>O (CO<sub>2</sub>/MDEA mole ratio: 0.15) is equal to that of HFC245fa and larger than that of water. The flow rate of

30 mass% MDEA-H<sub>2</sub>O (CO<sub>2</sub>/MDEA mole ratio: 0.15) is one-seventh as much as that of HFC245fa.

**Table 1.** Maximum power dependency on the fluid, flow rate, and expansion ratio

Fluid	Fluid Flow (kg/h)	Expansion Ratio	Power (kW)
30 mass% MDEA-H <sub>2</sub> O (CO <sub>2</sub> /MDEA mole ratio: 0)	5,000	3.3	139
30 mass% MDEA-H <sub>2</sub> O (CO <sub>2</sub> /MDEA mole ratio: 0.10)	5,000	3.3	139
30 mass% MDEA-H <sub>2</sub> O (CO <sub>2</sub> /MDEA mole ratio: 0.15)	6,000-7,000	3.3-3.5	151
30 mass% MDEA-H <sub>2</sub> O (CO <sub>2</sub> /MDEA mole ratio: 0.20)	8,000	2.9-3.1	141
20 mass% MDEA-H <sub>2</sub> O (CO <sub>2</sub> /MDEA mole ratio: 0.15)	4,500	3.3	145
25 mass% MDEA-H <sub>2</sub> O (CO <sub>2</sub> /MDEA mole ratio: 0.15)	4,750	3.5	148
35 mass% MDEA-H <sub>2</sub> O (CO <sub>2</sub> /MDEA mole ratio: 0.05)	5,500	3.4	142
15 mass% MEA-H <sub>2</sub> O	6,000	3.0	125
30 mass% MEA-H <sub>2</sub> O	6,000	3.0	114
H <sub>2</sub> O	3,200-3,400	3.2-3.0	132
HFC245fa	42,000-49,000	2.3-2.0	148

Therefore we consider the low temperature cycle using the 30 mass% MDEA-H<sub>2</sub>O (CO<sub>2</sub>/MDEA mole ratio: 0.15) is one of the alternatives to the Organic Rankine cycle using HFC245fa.

### 3.2 Experimental results

A MDEA-based solution is used as the fluid on the basis of the model predictions.

#### 3.2.1 CO<sub>2</sub>/amine solution volume ratio of 10 Nm<sup>3</sup>/m<sup>3</sup>

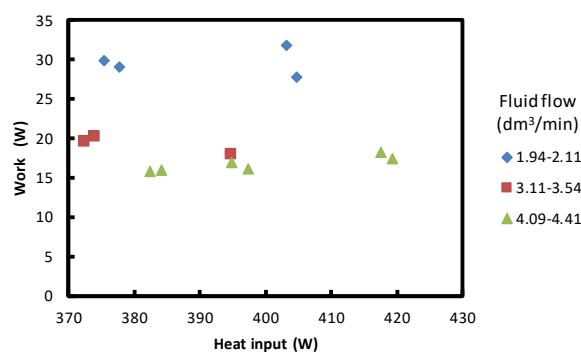
Figure 4 shows the work as a function of the heat input. The work is independent of the heat input.

Figure 5 shows the work and efficiency as a function of the fluid flow. The work and efficiency decreases with the fluid flow.

Figure 6 shows the flow of the generated steam and CO<sub>2</sub> as a function of the fluid flow. The flow of the generated steam decreases with the fluid flow. The flow of the generated CO<sub>2</sub> is independent to the fluid flow.

#### 3.2.2 CO<sub>2</sub>/amine solution volume ratio of 20 Nm<sup>3</sup>/m<sup>3</sup>

Figure 7 shows the work and efficiency as a function of the fluid flow. The maximum value of the efficiency was 10 percent. The work and efficiency decrease with the fluid flow.



**Figure 4.** Work as a function of heat input at CO<sub>2</sub>/amine solution volume ratio of 10 Nm<sup>3</sup>/m<sup>3</sup>

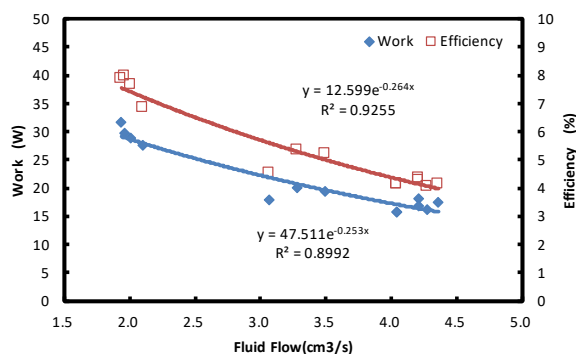


**Figure 5.** Work and efficiency as a function of fluid flow at CO<sub>2</sub>/amine solution volume ratio of 10 Nm<sup>3</sup>/m<sup>3</sup>

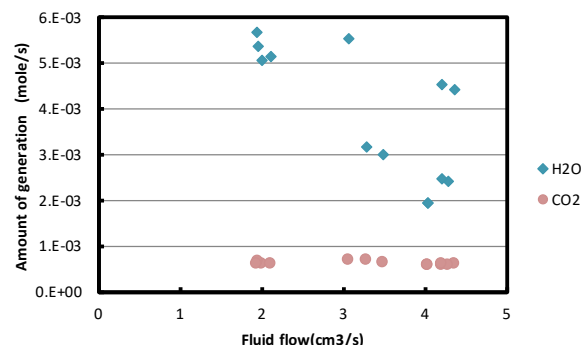


**Figure 6.** Amount of generation as a function of fluid flow at CO<sub>2</sub>/amine solution volume ratio of 10Nm<sup>3</sup>/m<sup>3</sup>

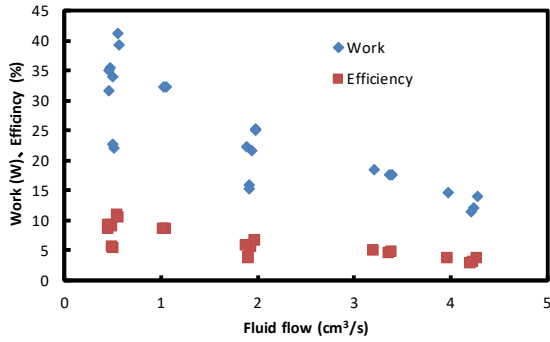


**Figure 7.** Work and Efficiency as a function of fluid flow at CO<sub>2</sub>/amine solution volume ratio of 20Nm<sup>3</sup>/m<sup>3</sup>

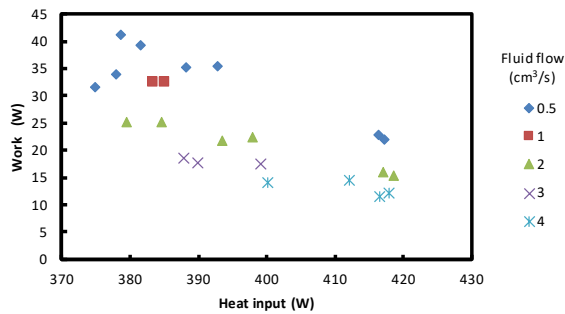


**Figure 8.** Work as functions of heat input and fluid flow at CO<sub>2</sub>/amine solution volume ratio of 20Nm<sup>3</sup>/m<sup>3</sup>

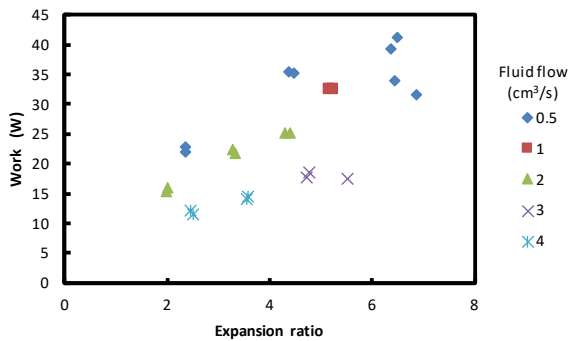


**Figure 9.** Work as functions of expansion ratio and fluid flow at CO<sub>2</sub>/amine solution volume ratio of 20Nm<sup>3</sup>/m<sup>3</sup>

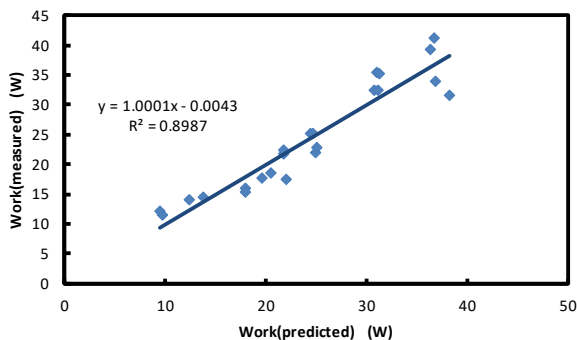


**Figure 10.** Work (measured) vs. Work(predicted) at CO<sub>2</sub>/amine solution volume ratio of 20Nm<sup>3</sup>/m<sup>3</sup>

Figure 8 shows the work as function of the heat input and fluid flow. The work decreases with the heat input.

Figure 9 shows the work as functions of the expansion ratio and fluid flow. The work increases with the expansion ratio.

A multiple regression equation approximating the work is obtained as follows:

$$W = 20.26 - 4.230F + 2.896ER \quad (4)$$

where  $W$  is the work (W),  $F$  is the fluid flow (cm<sup>3</sup>/s), and  $ER$  is the expansion ratio.

Figure 10 shows the measured work as a function of the work predicted using Eq. (4). The measured values of the work are in good agreement with the predicted values of the work. The predicted values of the work using Eq. (4) don't show good agreement with the measured values of the work at the CO<sub>2</sub>/amine solution volume ratio of 10Nm<sup>3</sup>/m<sup>3</sup>.

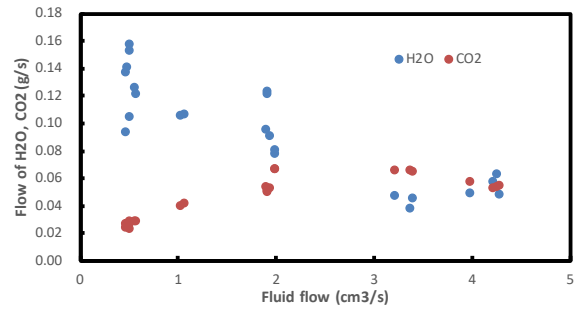


**Figure 11.** Flow of generated H<sub>2</sub>O and CO<sub>2</sub> as a function of fluid flow at CO<sub>2</sub>/amine solution volume ratio of 20Nm<sup>3</sup>/m<sup>3</sup>

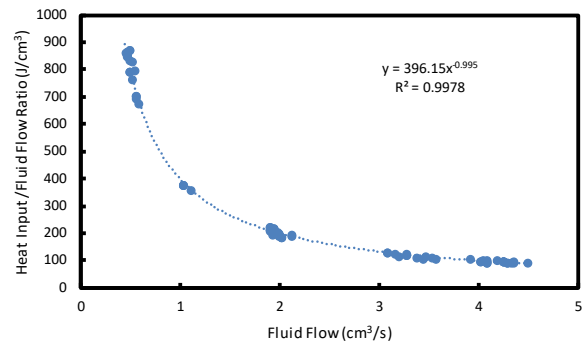


**Figure 12.** Heat input /fluid flow ratio as a function of fluid flow at CO<sub>2</sub>/amine solution volume ratio of 10 and 20Nm<sup>3</sup>/m<sup>3</sup>

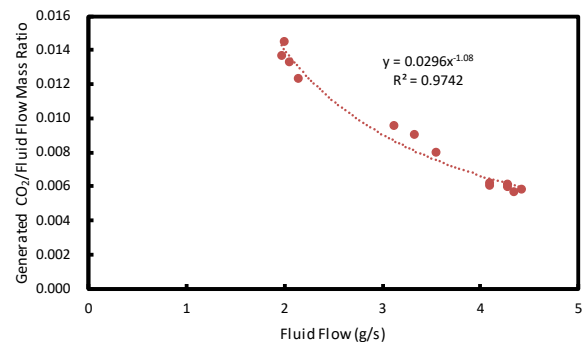


**Figure 13.** Heat input /fluid flow ratio as a function of fluid flow at CO<sub>2</sub>/amine solution volume ratio of 10Nm<sup>3</sup>/m<sup>3</sup>

Figure 11 shows the flow of the generated steam and CO<sub>2</sub> as a function of the fluid flow. The flow of the generated steam decreases with the fluid flow. The flow

of the generated CO<sub>2</sub> shows the maximum value at the fluid flow between 2–3 cm<sup>3</sup>/s.

### 3.3 Discussion

Figure 12 shows the heat input/fluid flow ratio as a function of the fluid flow. The heat input/fluid flow ratio is inversely proportional to the fluid flow. The works in Figures 5 and 7 and the generated H<sub>2</sub>O flows in Figures 6 and 11 decrease with the fluid flow similarly.

The present authors consider the heat for heating the fluid to the bubble point of the MDEA-based solution increases with the fluid flow. Therefore, the heat for generating steam and CO<sub>2</sub> decreases with the fluid flow under nearly constant heat input (about 400 W).

Figure 13 shows the generated CO<sub>2</sub>/fluid flow ratio as a function of the fluid flow at CO<sub>2</sub>/amine solution volume ratio of 10Nm<sup>3</sup>/m<sup>3</sup>. The generated CO<sub>2</sub>/fluid flow ratio decreases with the fluid flow in the same way the heat input/fluid flow ratio does in Figure 12. Therefore, the flow of the generated CO<sub>2</sub> is independent to the fluid flow at CO<sub>2</sub>/amine solution volume ratio of 10Nm<sup>3</sup>/m<sup>3</sup>.

## 4 Conclusion

The thermodynamic simulation of the low temperature cycle using 30 mass% MDEA-H<sub>2</sub>O solution (CO<sub>2</sub>/MDEA mole ratio: 0.15) is one of the alternatives to the organic Rankine cycle using HFC245fa.

The experimental results suggest that the low temperature cycle using the MDEA-based solution is available as a low temperature cycle.

## References

Akgiary, O. and A. M. Saatci; “A New Look at Filter Backwash Hydraulics,” *Water Sci. Technol.*, **38**, 89–96 (2001)

Ergun, S.; “Fluid Flow through Packed Columns,” *Chem. Eng. Prog.*, **48**, 89–94 (1952)

Myhre, G., D. Shindell, F.-M. Breon, W. Collins, J. Fuglestedt, J. Huang, D. Koch, J. -F. Lamarque, D. Lee, B. Mendoza, T. Nakajima, A. Robock, G. Stephens, T. Takamura, and H. Zheng; “Anthrogenic and Natural Radiative Forcing” in *Climate Change 2013: The Physical Science Basis Contribution of Working Group to the Fifth Assessment Report of the Intergovernmental Panel on Climate Change*, Stocker, T. F., D. Qin, G.-K. Plattner, M. Tignor, S. K. Allen, J. Boschung, A. Nauels, Y. Xia, V. Bex, and P. M. Midgley eds., Cambridge University Press, Cambridge, U.K. and New York, U.S.A. (2013)

Nishikawa, J. ed.; *Heat Engine*, pp.73, University of Tokyo Press, Tokyo, Japan (1965)

Ogawa, T., Y. Ohashi, S. Yamanaka, and K. Miyaike; “Development of Carbon Dioxide Removal System from the Flue Gas of Coal Fired Power Plant,” *Energy Procedia*, **1**, 721–724 (2008)

Shindo, T., Y. Nakatani, and T. Oishi; “Thermoelectric Generating System for Effective Use of Unutilized Energy,” *Toshiba Review*, **63**(2), 7-10 (2008)